Characterization of the Activities of Dinuclear Thiolato-Bridged Arene Ruthenium Complexes against *Toxoplasma gondii*

Afonso P. Basto,[a,‡] Joachim Müller,[a,‡] Riccardo Rubbiani,[b,‡] David Stibal,[d] Federico Giannini,[c] Georg Süss-Fink,[d] Vreni Balmer,[a] Andrew Hemphill,*[,a] Gilles Gasser,*[e] and Julien Furrer*[,c]

[a]*Institute of Parasitology, Vetsuisse Faculty, University of Bern, Länggassstrasse 122, CH-3012 Berne, Switzerland.*

[b]*Department of Chemistry, University of Zurich, Winterthurerstrasse 190, CH-8057 Zurich, Switzerland.*

[c]*Department for Chemistry and Biochemistry, Freiestrasse 3 CH-3012 Bern, Switzerland.*

[d]*Institut de Chimie, Université de Neuchâtel, Avenue de Bellevaux 51, CH-2000 Neuchâtel, Switzerland.*

[e]*Chimie ParisTech, PSL Research University, Laboratory for Inorganic Chemical Biology, F-75005 Paris, France.*

*Corresponding authors:

Chemistry:

Julien Furrer, Tel. +41 631 43 83; julien.furrer@dcb.unibe.ch

Gilles Gasser, Tel. +33 1 44 27 56 02 ; gilles.gasser@chimie-paristech.fr

Parasitology:

Andrew Hemphill, Tel. +41-31-6312384; Fax +41-31-6312477;

andrew.hemphill@vetsuisse.unibe.ch

[‡] All three authors contributed equally to the work

Abstract

The *in vitro* effects of 18 dinuclear-thiolato bridged arene ruthenium complexes, (1 mono-, 4 di- and 13-tri-thiolato compounds), originally designed as anti-cancer agents, were studied in the apicomplexan parasite *Toxoplasma gondii* grown in human foreskin fibroblast host cells (HFF). Some tri-thiolato compounds exhibited anti-parasitic efficacy at 250 nM and below. Among those, complex 1 and complex 2 inhibited *T. gondii* proliferation with IC_{50} values of 34 and 62 nM, respectively, and they did not affect HFF at dosages of 200 µM or above, resulting in selectivity indices of > 23'000. The IC_{50} values of complex 9 were 1.2 nM for *T. gondii* and above 5 µM for HFF. TEM detected ultrastructural alterations in the matrix of the parasite mitochondria at the early stages of treatment, followed by more pronounced destruction of tachyzoites. However, all three compounds applied at 250 nM for 15 days were not parasiticidal. By affinity chromatography using complex 9 coupled to epoxy-activated sepharose followed by mass spectrometry, *T. gondii* translation elongation factor-1 alpha and two ribosomal proteins, RPS18, and RPL27 were identified as potential binding proteins. In conclusion, organometallic ruthenium complexes exhibit promising activities against *Toxoplasma*, and potential mechanisms of action of these compounds as well as their prospective applications for the treatment of toxoplasmosis are discussed.

INTRODUCTION

Organometallic compounds, especially platinum complexes, are widely applied as anti-cancer chemotherapeutics (1). However, due to their drawbacks (i.e. severe side effects, insurgence of tumor resistance, etc.), a variety of complexes of other transition metals such as copper, gold or ruthenium have been investigated as potential alternative anti-cancer drug candidates (2-10). Among the different metal complexes studied, arene ruthenium complexes showed very promising anti-cancer properties with 50% inhibitory concentration (IC_{50}) values in the low micromolar range, and certain selectivity for tumor cells over non-tumorigenic cells (11-13). One such compound, namely RAPTA-C, is currently in pre-clinical evaluation (14). Recently, some of us have shown that thiolato-bridged dinuclear arene ruthenium complexes, in particular trithiolato dinuclear complexes of the type $[(\eta^6\text{-}p\text{-}MeC_6H_4Pr^i)_2Ru_2(\mu_2\text{-}SR)_3]^+$ and $[(\eta^6\text{-}p\text{-}MeC_6H_4Pr^i)_2Ru_2(\mu_2\text{-}SR^1)(\mu_2\text{-}SR^2)_2]^+$, were among the most cytotoxic ruthenium complexes reported so far, with nanomolar IC_{50} values against both A2780 human ovarian cancer cells and their cisplatin-resistant mutant variant A2780cisR (15-21). Interestingly, *in vivo* studies on one of these compounds, namely $[(\eta^6\text{-}p\text{-}MeC_6H_4Pr^i)_2Ru_2(\mu_2\text{-}SC_6H_4\text{-}p\text{-}Bu^t)_3]^+$ (*diruthenium-1*) demonstrated a significant increase in survival of treated mice (22).

Arene ruthenium complexes also showed to be effective against bacteria (23), against protozoan parasites including the two closely related apicomplexans *Neospora caninum* and *Toxoplasma gondii*(24) and against helminths such as *Schistosoma mansoni* (25, 26) and *Echinococcus multilocularis* (27). Interestingly, some ruthenium-clotrimazole (ctz) complexes displayed high *in vitro* activity against *Leishmania major* and *Trypanosoma cruzi* and low toxicity when assessed in normal mammalian cells (28). In addition to ruthenium, other organometallic complexes have also been reported to display interesting anti-parasitic or/and anti-infective activities (29-42). For instance, one manganese(I) tricarbonyl complex, $[Mn(CO)_3(bpy^{R,R})(ctz)]PF_{6,}$, showed submicromolar activity against *Staphylococcus aureus*

and *S. epidermidis* with minimum inhibitory concentrations (MICs) of 0.625 μM. Moreover, the related complex $[Mn(CO)_3(bpy^{R,R})(ktz)]PF_6$, (ktz = ketoconazole) was active against *Trypanosoma brucei* with an IC_{50} value of 0.7 μM, while the IC_{50} value in mammalian cells was more than 10 times higher (43).

Among the different above-mentioned pathogens, *T. gondii* is the most widespread parasite worldwide, and infects approximately one third of the human population (44). In general, *T. gondii* infestation remains without clinical symptoms in immune competent individuals, and no treatment is required. However, *Toxoplasma* infection has been linked to neuropsychiatric disease. Importantly, upon immunosuppression, or primary infection during pregnancy, *T. gondii* can cause toxoplasmosis, a life-threatening disease affecting both humans but also food and farm animals, which can lead to severe pathology including fetal malformation and abortion. Current treatment options for toxoplasmosis include macrolide antibiotics and sulfonamides (45), which inhibit protein biosynthesis and intermediary metabolism in the apicoplast, a prokaryote-like organelle that is unique to apicomplexans (46). However, these treatments are often characterized by adverse side effects, and do not eliminate the parasite, thus do not act in a parasiticidal manner. It is therefore of high interest to investigate whether dinuclear thiolato-bridged arene ruthenium complexes exhibit selective toxicity and parasiticidal activity against *T. gondii*. Moreover, compounds with good efficacy against *T. gondii* have good chances of being active against related apicomplexan parasites of high medical and veterinary medical interest such as the coccidians *Cryptosporidium* and *Eimeria*, and the closely related *Neospora caninum.*

MATERIALS AND METHODS

Chemicals and synthesis of ruthenium complexes. All reagents were commercially available and were used as received. The complexes assessed in this study are shown in Fig.

1. The symmetrical trithiolato complexes 1-7 were synthesized following a slightly modified published protocol (17). The dinuclear complex $[(\eta^6\text{-}p\text{-}MeC_6H_4Pr^i)Ru_2(\mu\text{-}Cl)Cl_2]$ was first dissolved and heated in refluxing technical grade ethanol, and a solution of 6 equivalents of the corresponding thiol SR in 5 mL technical grade ethanol EtOH was added dropwise (R = 4-$C_6H_4CH_3$: 1; 4-$C_6H_4Bu^t$: 2; 4-C_6H_4OH: 3; 3,4-$C_6H_3(OMe)_2$: 4; 4-mco, mco = methylcoumarinyl: 5; 3-C_6H_4Cl: 6; 3-$C_6H_4NH_2$: 7). The resulting mixture was refluxed for 18 h. After cooling to room temperature, the solvent was removed under reduced pressure. The oil obtained was purified by column chromatography on silica gel using a mixture of dichloromethane and ethanol (5:1) as the eluent. The "mixed" trithiolato complexes 8-13 were synthesized in two steps, as previously described (19, 47). First, the neutral dichlorido dithiolato intermediates $[(\eta^6\text{-}p\text{-}MeC_6H_4Pr^i)_2Ru_2(\mu_2\text{-}SCH_2\text{-}C_6H_4\text{-}R)_2Cl_2]$ are obtained from the reaction of the *p*-cymene ruthenium dichloride dimer $[(\eta^6\text{-}p\text{-}MeC_6H_4Pr^i)Ru_2(\mu\text{-}Cl)Cl_2]$ with 2 equivalents of the respective thiol SCH_2R (R = C_6H_5: 8; R = 4-$C_6H_4CH_3$: 9; R = 4-C_6H_4OMe: 10; R = 4-C_6H_4F: 11; R = 4-C_6H_4Cl: 12; R = 4-C_6H_4Br: 13 in ethanol at 0 °C, according to the published method (49). These intermediates react in refluxing ethanol during 15 h with 6 equivalents of 4-Mercaptophenol 4-HS-C_6H_4-OH to give the corresponding mixed trithiolato complexes $[(\eta^6\text{-}p\text{-}MeC_6H_4Pr^i)_2Ru_2(\mu_2\text{-}S\text{-}C_6H_4\text{-}OH)(\mu_2\text{-}SR)_2]^+$ 8-13. The dithiolato complexes 14-17 and the monothiolato complex 18 were synthesized according to published methods (48, 49). The resulting complexes 1 – 18 (Fig. 1,) which were isolated as chloride or tetrafluoroborate salts are air-stable, orange to red solids and were dried in vacuum. The analytical data matched those previously reported in the literature (15, 17, 47, 48).

Host cell cultivation and parasite cultures. If not stated otherwise, all tissue culture media were purchased from Gibco-BRL (Zurich, Switzerland), and biochemical reagents were from Sigma (St. Louis, MO). Human foreskin fibroblasts (HFF) and Vero cells (green monkey kidney epithelial cells) were maintained in RPMI-medium containing 10% fetal calf serum (FCS) (Gibco-BRL, Zürich, Switzerland) and antibiotics as described earlier (24). *T. gondii*

beta-gal (transgenic *T. gondii* RH expressing the beta-galactosidase gene from *E. coli* (50)) were maintained in Vero cells, and were isolated and separated from their host cells as described (24).

***In vitro* assessment of drug efficacy.** To study the effects of compounds against *T. gondii* tachyzoites *in vitro*, 0.5 mM stock solutions of complexes were prepared in water, sterile filtered, and stored at 4 °C.

For assessment of drug efficacy against *T. gondii* tachyzoites, parasites were isolated (24) and assays were performed using HFF as host cells (24). In short, 5 x 10^3 HFF cells / well) were grown to confluence in a 96 well plate in phenol-red free culture medium at 37 °C with 5% CO_2. Cultures were infected with freshly isolated *T. gondii* beta-gal tachyzoites beta-gal tachyzoites (1 x 10^3 / well) and drugs were added at the time point of infection. Initial assessments of drug efficacy were done by exposing parasite cultures to 2500 nM, 250 nM, 25 nM or 2.5 nM of each compound for a period of three days, or water was added as a control. For IC_{50} determinations, 6 selected complexes (1-5, and 9) were added at concentrations ranging between 0 and 2000 nM. After three days at 37 °C/ 5% CO_2, plates were centrifuged at 500 g, medium was removed, and cell cultures were lysed in PBS containing 0.05% Triton-X-100. After addition of 10 µL of 5 mM chlorophenol red-β-D-galactopyranoside (CPRG; Roche Diagnostics, Rotkreuz, Switzerland) dissolved in PBS, the absorption shift was measured at 570 nm wavelength at various time points on a VersaMax multiplate reader (Bucher Biotec, Basel, Switzerland). The activity, measured as the release of chlorophenol red over time, was proportional to the number of live parasites down to 50 per well as determined in pilot assays. IC_{50} values were calculated after the logit-log-transformation of relative growth and subsequent regression analysis by the corresponding software tool contained in the Excel software package (Microsoft, Seattle, WA).

143 In one time course experiment, 9 (100 nM) was added to HFF monolayers either 10 min prior
144 to infection or 1 h, 5 h or 24 h post-infection with *T. gondii* tachyzoites. The proliferation of
145 tachyzoites was measured after 2 days of culture as described above.

146 For long term treatment assays, *T. gondii* infected HFF grown in T25 culture flasks were
147 exposed to 250 nM of 1, 2 or 9 for a period of 15 days, after which the cultures were washed
148 with medium and were further maintained in medium devoid of drugs. Regrowth of parasites
149 was monitored on a daily basis by light microscopy

150 Cytotoxicity assays on non-infected confluent HFF were performed also in 96 well plates by
151 exposing HFF to a concentration range of 2.5 nM, 25 nM, 250 nM and 2.5 µM of each
152 compound, and assessment of the viability by AlamarBlue assay as described (51).

153 **Transmission electron microscopy (TEM).** HFF (5 x 10^4 per inoculum) cultured in T25
154 tissue culture flasks for 24 h were infected with 10^5 *T. gondii* beta-gal tachyzoites, and 200
155 nM of 1, 2 or 9 were added at 24 h post-infection. After 6, 24 or 48 h, cells were harvested
156 using a cell scraper, and they were placed into the primary fixation solution (2.5 %
157 glutaraldehyde in 100 mM sodium cacodylate buffer pH 7.3) for 2 h. Specimens were then
158 washed 2 times in cacodylate buffer and were post-fixed in 2% OsO4 in cacodylate buffer for
159 2 h, followed by washing in water, pre-staining in saturated uranyle acetate solution, and step
160 wise dehydration in ethanol. They were then embedded in Epon 812-resin, and processed for
161 TEM as described (24). Specimens were viewed on a Phillips 400 transmission electron
162 microscope operating at 80 kV.

163 **Coupling of compound 9 to epoxy-activated sepharose, affinity chromatography and**
164 **identification of a drug-binding protein by liquid chromatography tandem mass**
165 **spectrometry (LC–MS/MS) analysis.** To prepare a complex-9-sepharose matrix, 20 mg of
166 complex 9 were added to 0.5 mg of epoxy-sepharose suspended in 2 mL of coupling buffer
167 ($NaCO_3$ 0.1 M, pH 9.5) followed by an incubation for two days at 37 °C on a shaker.

168 Furthermore, a mock epoxy-sepharose column was prepared by treatment with coupling
169 buffer without complex 9 and blocking with ethanolamine. Prior to the runs, both columns
170 were combined in a tandem (mock column first, then complex-9-column) and washed with 25
171 mL of PBS equilibrated at 20 °C.

172 To identify potential binding proteins both from *T. gondii* and from the host cell, three T75-
173 flasks containing HFF monolayers were infected with 2 x 10^7 *T. gondii* tachyzoites and
174 incubated for 3-4 days. Then, cells were harvested by scraping and pelleted (1,000 g, 10 min,
175 4◦C). For protein extraction, frozen pellets were resuspended in 1 ml ice cold PBS containing
176 1% Triton-X-100 and 1 mM phenyl-methyl-sulfonyl-fluoride. Suspensions were vortexed
177 thoroughly, and centrifuged (15,200 x g), 10 min, 4◦C). Extraction of pellets was repeated
178 twice. Supernatants were combined (5–10 mg of total protein) and subjected to affinity
179 chromatography by loading onto the column tandem at a flow rate of 0.25 mL/min. The
180 columns were washed with PBS until a flat baseline was detected (ca. 20 mL PBS). The
181 columns were separated, and proteins binding to the columns were eluted with a pH shift
182 (glycine Cl^- 100 mM, pH 2.9). Fractions (3 mL) were taken before, during and after elution
183 and precipitated overnight with 80% acetone at –20 °C. The precipitates were solubilized in
184 30 µL of Laemmli buffer and were separated by 10% sodium dodecyl sulphate
185 polyacrylamide gelelectrophoresis (SDS-PAGE) using a Hoefer Minigel 250 Apparatus (GE
186 Healthcare, Little Chalfont, UK). Proteins were visualized by silver staining.

187 For mass spectrometry analysis, colloidal Coomassie staining was applied and selected
188 protein bands were cut out with a clean scalpel, placed into Eppendorf tubes containing
189 ethanol/distilled water (1:4) and were stored at 4 °C. In-gel digestion/liquid chromatography
190 tandem mass spectrometry (LC–MS/MS) analysis was performed by the Mass Spectrometry
191 and Proteomics Facility at the Department of Clinical Research of the University of Bern
192 (Bern, Switzerland). The sequences obtained were blasted against the UniProt database
193 (www.uniprot.org).

RESULTS

***In vitro* efficacy of Ru(II) complexes.** The tri-thiolato complexes 1-5 and the mixed complex 9 inhibited the proliferation of *T. gondii* with IC_{50} values of approximatively 500 nM or below (Table 1). The tri-thiolato complex 7 and the mixed complexes 8 and 10-13 had no measurable anti-parasitic activity or were toxic for host cells already at concentrations of 250 nM or 2500 nM. The same was true for the di-thiolato complexes 14-17 and the mono-thiolato complex 18. The activity of the complexes against *T. gondii* parallels to a certain extent the results previously found against several cancer cell lines: the IC_{50} values of 7 were two orders of magnitude larger than that of the other complexes (20), and the mono- and dithiolato complexes were found to be only moderately cytotoxic in vitro against cancer cell lines (IC_{50} values between 0.2 and 2.5 µM) (48, 49).

Complexes 1, 2 and 9 appeared as the most active with IC_{50} values of 34, 62 and 1.2 nM, respectively (see Table 1). Accordingly, host cell toxicity was investigated for these three complexes. In the presence of 1, HFF vitality was decreased to 63% of the control value at a concentration of 250µM, which was the highest concentration used in these assays. Thus, an extrapolated, but purely theoretical, IC_{50} value of 800 µM was calculated for 1, since the solubility limit in water-based solutions is around 500 µM. 2 did not affect vitality of HFF up to a concentration of 250 µM. 9, exhibiting the by far lowest IC_{50} values, had an IC_{50} for HFF of approximately 5 µM. Thus, all three complexes affected *T. gondii* tachyzoites at low nanomolar concentrations, and these effects were parasite-specific, with a high selective toxicity index: > 23,000 for 1, > 16,000 for 2, and > 5,000 for 9. Interestingly, a long-term treatment with compound 9 at 250 nM 9 over a period of up to 15 days did not eliminate all parasites, since regrowth of tachyzoites was observed 5-10 days after releasing drug pressure

for all three compounds. This indicates that these compounds acted in a parasitostatic rather than parasiticidal manner.

Ultrastructural changes induced by Ru(II) complexes show that one of the primary target organelles in *T. gondii* tachyzoites is the mitochondrion. To obtain more detailed information on the subcellular effects of these 3 thiolato-bridged dinuclear arene ruthenium complexes, TEM was performed on drug-treated HFF infected with *T. gondii* (Fig. 2, 3). Non-treated parasites, exemplified in Fig. 2 were located intracellularly and were undergoing proliferation by endodyogeny within a parasitophorous vacuole (PV), surrounded by a distinct PV membrane. These parasites exhibit the typical apicomplexan structural features, including rhoptries, dense granules, micronemes, and a conoid at the anterior part. The parasite mitochondrium, filled with a structured electron dense matrix, could be readily identified in these non-treated parasites (Fig. 2C). In cultures exposed to 1, alterations within the mitochondria of *T. gondii* were evident already after 6 h of treatment, showing a progressive degeneration of the electron-dense intra-mitochondrial matrix (Fig. 3B-C). The interior ultrastructural organization of these mitochondria was largely distorted and only membranous residues were present in some cases. However, the outer membrane of the mitochondria was still intact, and parasites maintained their overall shape. After 48 h of treatment with 1, *T. gondii* tachyzoites had lost their characteristic shape, and parasites displayed a largely distorted morphology, no internal organelles were recognizable anymore, and the PV and its membrane were essentially lost. However, host cell mitochondria exhibited a normal morphology with clearly discernable cristae (Fig. 3D). Similar results were obtained in *T. gondii* infected cultures treated with 2 (data not shown). For treatments with 9, mitochondrial changes were not noted in *T. gondii* tachzyoites already after 6 h of treatment (data not shown), but similar alterations as observed during treatments with 1 became evident after 24-48 h of 9 exposure (Fig. 3E, F). However, intact parasites could also be observed in cultures treated with all three complexes. Overall, this suggested that these three ruthenium complexes

induced largely similar ultrastructural changes by inducing distinct alterations in the mitochondria, and could thus act with (a) similar or identical mechanism(s) of action.

Complex 9 affects extracellular parasites and interferes in adhesion, invasion or intracellular establishment, but does not act efficiently against *T. gondii* proliferation once parasites reside inside the host cell. Since long-term treatment studies as well as TEM suggested that these ruthenium complexes did not act parasiticidal, we wanted to determine whether these compounds affected host cell invasion, intracellular proliferation, or both. For this, HFF monolayers were infected with *T. gondii* tachyzoites, and 9 (100 µM) was added either concomitantly with the infection, or after 1 h, 5 h or 24 h post infection (Fig. 4). 9 efficiently inhibited tachyzoite proliferation when added at the time point of infection and also when applied at 5 h post-infection, but only partially when added 24 h post-infection. Thus 9 acted mainly during first steps of the infection process (e.g. host cell invasion and intracellular establishment), and only with limited efficacy once parasites resided inside the host cell.

Complex 9 interacts with ribosomal proteins from *T. gondii* and from the host cell. By affinity chromatography on complex-9-epoxy-sepharose, two major bands of approximately 50 kDa and 20 kDa were identified that were not present in the eluate of the mock column (Fig. 5 A). Mass spectrometry analysis identified ribosomal proteins of host and parasite origin as major components of the 20-kDa-band (Table 1). The composition of the 50 kDa band was more heterogeneous. As quantified both via protein match score summation and via protein score – the major component of the 50 kDa-band was *T. gondii* elongation factor 1-alpha (TgEF1-alpha; Table 1) with a unique peptide coverage of nearly 50% of the sequence (Fig. 5B). The second most abundant protein was its human homologue. Moreover, other proteins of human origin were identified in this fraction (Table 1).

DISCUSSION

We here report on a series of 18 dinuclear thiophenolato-bridged arene ruthenium complexes, which exhibit highly promising *in vitro* activities against *T. gondii* tachyzoites. The organometallic complexes studied in this work have been previously described (15, 17, 47, 48). Very importantly, recent studies by some of us have shown that these dinuclear arene ruthenium complexes are inert to ligand substitutions and remain stable for long period in water solutions or in organic solvents like DMSO (16, 21). These ruthenium complexes had been originally generated for the treatment of cancer cells. Cancer cells and protozoan parasites, including *Toxoplasma*, share several features: they both live and multiply in a host organism and do not immediately kill their hosts, they have a potentially infinite proliferative capacity, and escape in immune-compromised tissues. Cancer cells are largely resistant to apoptosis, while *Toxoplasma* and *Neospora* are known to interfere in the programmed cell death machinery of their host cell (52). Thus, we hypothesize that a potentially lucrative starting point for the discovery of novel drug candidates against *T. gondii* and other protozoans is to examine compounds that are being developed against cancer.

Among the 18 compounds studied, the trithiolato complexes 1, 2 and 9 were highly efficacious against both parasites with IC_{50}s ranging between 1.2 and 62 nM. In addition, these compounds exhibited a highly favorable selective toxicity index of up to 23'000. TEM demonstrated that one of the first organelles that exhibited ultrastructural alterations upon treatment with these compounds was the tachyzoite mitochondrion, which lost its interior membranous matrix and cristae already after 6-24 h. More severe distortion, including a complete breakdown of other organelles within the parasite cytoplasm and a general disintegration of the tachzoites and the parasitophorous vacuole and its membrane, was observed after 48 h.

In comparison to other drugs, the *in vitro* results on complexes 1, 2 and 9 are encouraging. Pyrimethamine, sulfadiazine and atovaquone, compounds currently clinically used against

toxoplasmosis, inhibited *T. gondii* beta-gal with IC_{50} values of 1 mM, 80 µM and 19-50 nM, respectively (50). The calcium dependent protein kinase inhibitor BKI-1294, highly active against *T. gondii* and *N. caninum* infections in mice, inhibited *T. gondii* and *N. caninum* beta-gal proliferation under identical conditions with an IC_{50} of 137 and 40 nM, respectively (53). Two previously identified organometallic ruthenium complexes exhibited IC_{50} values of 18 and 41 nM (24) however, with selective toxicity indeces below 100. As can be noticed from the calculated Log P values (Table 1) and as previously observed against cancer cells (17), the efficacy of inhibition is, to some extent, correlated to the lipophilicity of the complexes. Unlike against A2780 and A2780cisR cancer cells, the most lipophilic complex, 2, is not the most potent one against *T. gondii*, possibly suggesting that the different chemical nature of the cell and *T. gondii* outer membranes could influence the uptake of dinuclear thiolato-bridged arene ruthenium complexes.

While 1, 2 and 9 were highly efficacious against *T. gondii* and exhibited an excellent selective toxicity, we obtained evidence that these compounds did not act in a parasiticidal manner. Removal of the drugs after continuous treatments at 250 nM lasting up to 15 days did not result in complete elimination of viable tachyzoites, and re-growth of parasites was observed within 5-10 days after releasing the drug pressure. This was confirmed by TEM, where a small number of largely intact tachyzoites were still found after 48 h of continuous *in vitro* treatment. Similar results were previously reported for dicationic arylimidamides (54) and ruthenium phosphite complexes in *T. gondii* (24), and for buparvaquone, the BKI-1294 as well as for artemisinin derivatives in the closely related *N. caninum* (55-57). In some of these reports, rapid adaptation of *T. gondii* and *N. caninum* tachyzoites to increased concentrations of drugs within a few days was documented (54, 56). This outstanding adaptive ability represents a major obstacle for the development of efficacious drugs against these parasites. Nevertheless, the lack of parasiticidal activity *in vitro* still allows for excellent *in vivo*

efficacy, as documented for the BKI-1294 in pregnant murine infection models for *N. caninum* (55, 57).

All three compounds had a profound impact on the ultrastructure of the parasite mitochondria, which lost their characteristic electron dense matrix and cristae upon 6-24 h after initiation of drug treatments. After 48 h, this impacted on the entire tachyzoites, leading in most cases to severe alterations and death. Of note, mitochondria are also targeted by other drugs currently used against apicomplexans, such as atovaquone, buparvaquone and decoquinate, which have been shown to impair cytochrome b/c1 complex in *Toxoplasma, Plasmodium* and *Theileria* parasites (58-61).

The mitochondrion represents an attractive drug target. The disruption of mitochondria has been recently investigated as a potential novel chemotherapeutic mechanism for cancer treatment, because it circumvents upstream apoptotic pathways that may be mutated or lacking in cancer cells (62). Moreover, cancer cells have higher mitochondrial membrane potentials, rendering them more susceptible to mitochondrial perturbations than non-immortalized cells (63). On the basis of these factors, numerous mitochondria-targeting agents have been developed in order to disrupt the mitochondrial membrane potential and to further permeabilize the mitochondrial outer membrane. Some ruthenium(II) complexes can induce mitochondria–mediated apoptosis in cancer cells (64-67). However, while in mammalian cells the mitochondrion represents the main ATP-generating organelle that allows complete oxidation of carbohydrates, lipids and amino acids via the tricarboxylic acid (TCA) cycle and the electron transport chain, the situation in apicomplexans appears slightly different. Apicomplexans have a single tubular mitochondrial network that also hosts part of the heme biosynthesis, iron-sulfur cluster assembly, and lipoic acid salvage, and the mitochondrion participates in the synthesis of many metabolic intermediates including pyrimidines (68)

How exactly the mitochondrion is targeted by our ruthenium complexes is not known. Affinity chromatography using extracts from *T. gondii*-infected HFF lead to the identification of TgEF1-alpha as well as its human homologue as major complex-3-binding partners. This is not surprising since EF1-alpha is expressed in all eukaryotic cells and is highly conserved (69). In eukaryotic cells, EF1-alpha promotes the GTP-dependent transfer of aminoacylated tRNA to the ribosome A site, hence represents an essential component of protein synthesis. In addition, other activities have been attributed to EF1-alpha in different eukaryotes, which are associated with vital cellular functions such as cell growth, motility, protein metabolism, signal transduction, DNA replication/repair protein networks and apoptosis (70-72). In *Trypanosoma brucei* and *T. gondii,* EF1-alpha mediates the specificity of mitochondrial t-RNA import (73, 74) and disruption of this process could lead to the observed mitochondrial alterations.

In another apicomplexan parasite, *Cryptosporidium parvum*, CpEF1-alpha was shown to localize to the apical region of *C. parvum* sporozoites, and antibodies directed against CpTEF1-apha inhibited host cell invasion (75). The same was shown for *T. gondii* (76) Our study also showed that complex 9 had a profound efficacy when applied at the early stages of host cell infection, namely either during, or 1-5 h after, exposure of *T. gondii* tachyzoites to host cells, but more limited efficacy was noted when added 24 h after infection. This would be consistent with a mode of action that is relevant for invasion or early host cell establishment. In addition, vaccination of mice with recombinant TgEF1-1alpha and a DNA vaccine coding for TgEF1-alpha lead to significantly prolonged survival times in *T. gondii* infected mice (76, 77) underlining the importance of TgEF1-alpha for the infection process.

As outlined in Table 1, other ribosomal proteins both of host and parasite origin, and various other host proteins, were found to bind to 9 as well. This may explain the low, but still detectable, host cell toxicity of 9.

In conclusion, we have identified three promising dinuclear thiolato-bridged arene ruthenium complexes with promising and highly specific anti-parasitic activity, as assessed against *T. gondii*. These complexes induce severe mitochondrial alterations within 6-24 h of drug treatment, efficiently inhibit proliferation, but do not act in a parasiticical manner. One of these complexes, compound 9, interacts with TgTEF1-alpha and other parasite and host ribosomal proteins. Further studies will focus on the interactions of 9 and other promising ruthenium complexes with putative apicomplexan drug targets, and on the use of these drugs *in vivo*.

ACKNOWLEDGEMENTS

We acknowledge financial support by the Swiss National Science Foundation (SNSF Professorships N° PP00P2_133568 and PP00P2_157545 (GG), SNSF grants N° 310030_165782 (AH) and CRSII5_173718 (JF, AH, GG), the University of Bern (UniBe-ID; JF, AH), the University of Zurich (G.G), the Stiftung für wissenschaftliche Forschung of the University of Zurich (G.G.), the UBS Promedica Stiftung (R.R., G.G.), the Forschungskredit of the University of Zurich (R.R.), the Novartis Jubilee Foundation (R.R. G.G.). This work has received support under the program «Investissements d'Avenir » launched by the French Government and implemented by the ANR with the reference ANR-10-IDEX-0001-02 PSL (G.G.). Many thanks are addressed to David Sibley (Washington University, St. Louis, USA) for providing us with *T. gondii*-beta gal tachyzoites for screening purposes.

REFERENCES

1. Shaili E. 2014. Platinum anticancer drugs and photochemotherapeutic agents: recent advances and future developments. Science progress 97:20-40. 10.3184/003685014x13904811808460
2. Zhang CX, Lippard SJ. 2003. New metal complexes as potential therapeutics. Curr Opin Chem Biol 7:481-489. 10.1016/s1367-5931(03)00081-4
3. Ott I, Gust R. 2007. Preclinical and Clinical Studies on the Use of Platinum Complexes for Breast Cancer Treatment. Anti-Cancer Agents Med Chem 7:95-110. 10.2174/187152007779314071
4. Ronconi L, Sadler PJ. 2007. Using coordination chemistry to design new medicines. Coord Chem Rev 251:1633-1648. http://dx.doi.org/10.1016/j.ccr.2006.11.017
5. Bruijnincx PCA, Sadler PJ. 2008. New trends for metal complexes with anticancer activity. Curr Opin Chem Biol 12:197-206. 10.1016/j.cbpa.2007.11.013
6. Meggers E. 2009. Targeting proteins with metal complexes. Chem Commun (Cambridge, U K):1001-1010. 10.1039/b813568a
7. Gasser G, Ott I, Metzler-Nolte N. 2011. Organometallic Anticancer Compounds. J Med Chem 54:3-25. 10.1021/jm100020w
8. Sava G, Bergamo A, Dyson PJ. 2011. Metal-based antitumour drugs in the post-genomic era: what comes next? Dalton Trans 40:9069-9075. 10.1039/c1dt10522a
9. Hartinger CG, Metzler-Nolte N, Dyson PJ. 2012. Challenges and Opportunities in the Development of Organometallic Anticancer Drugs. Organometallics 31:5677-5685. 10.1021/om300373t
10. Komeda S, Casini A. 2012. Next-Generation Anticancer Metallodrugs. Current Topics in Medicinal Chemistry 12:219-235. 10.2174/156802612799078964
11. Casini A, Gabbiani C, Sorrentino F, Rigobello MP, Bindoli A, Geldbach TJ, Marrone A, Re N, Hartinger CG, Dyson PJ, Messori L. 2008. Emerging Protein Targets for Anticancer Metallodrugs: Inhibition of Thioredoxin Reductase and Cathepsin B by Antitumor Ruthenium(II)−Arene Compounds. J Med Chem 51:6773-6781. 10.1021/jm8006678
12. Oehninger L, Stefanopoulou M, Alborzinia H, Schur J, Ludewig S, Namikawa K, Munoz-Castro A, Koster RW, Baumann K, Wolfl S, Sheldrick WS, Ott I. 2013. Evaluation of arene ruthenium(ii) N-heterocyclic carbene complexes as organometallics interacting with thiol and selenol containing biomolecules. Dalton Trans 42:1657-1666. 10.1039/c2dt32319b
13. Clavel CM, Păunescu E, Nowak-Sliwinska P, Griffioen AW, Scopelliti R, Dyson PJ. 2014. Discovery of a Highly Tumor-Selective Organometallic Ruthenium(II)–Arene Complex. J Med Chem 57:3546-3558. 10.1021/jm5002748
14. Murray BS, Babak MV, Hartinger CG, Dyson PJ. 2016. The development of RAPTA compounds for the treatment of tumors. Coord Chem Rev 306, Part 1:86-114. http://dx.doi.org/10.1016/j.ccr.2015.06.014
15. Gras M, Therrien B, Süss-Fink G, Zava O, Dyson PJ. 2010. Thiophenolato-bridged dinuclear arene ruthenium complexes: a new family of highly cytotoxic anticancer agents. Dalton Trans 39:10305-10313. 10.1039/c0dt00887g
16. Giannini F, Süss-Fink G, Furrer J. 2011. Efficient Oxidation of Cysteine and Glutathione Catalyzed by a Dinuclear Areneruthenium Trithiolato Anticancer Complex. Inorg Chem 50:10552-10554. 10.1021/ic201941j
17. Giannini F, Furrer J, Ibao A-F, Süss-Fink G, Therrien B, Zava O, Baquie M, Dyson PJ, Stepnicka P. 2012. Highly cytotoxic trithiophenolatodiruthenium complexes of the type (eta(6)-p-MeC6H4Pr (i))(2)Ru-2(SC6H4-p-X)(3) (+): synthesis, molecular

structure, electrochemistry, cytotoxicity, and glutathione oxidation potential. J Biol Inorg Chem 17:951-960. 10.1007/s00775-012-0911-2

18. Giannini F, Paul LEH, Furrer J. 2012. Insights into the Mechanism of Action and Cellular Targets of Ruthenium Complexes from NMR Spectroscopy. Chimia 66:775-780. 10.2533/chimia.2012.775

19. Giannini F, Furrer J, Süss-Fink G, Clavel CM, Dyson PJ. 2013. Synthesis, characterization and in vitro anticancer activity of highly cytotoxic trithiolato diruthenium complexes of the type (eta(6)-p-(MeC6H4Pr)-Pr-i)(2)Ru-2(mu(2)-SR1)(2)(mu(2)-SR2) (+) containing different thiolato bridges. J Organomet Chem 744:41-48. 10.1016/j.jorganchem.2013.04.049

20. Giannini F, Paul LEH, Furrer J, Therrien B, Süss-Fink G. 2013. Highly cytotoxic diruthenium trithiolato complexes of the type (eta(6)-p-MeC6H4Pri)(2)Ru-2(mu(2)-SR)(3) (+): synthesis, characterization, molecular structure and in vitro anticancer activity. New J Chem 37:3503-3511. 10.1039/c3nj00476g

21. Furrer J, Süss-Fink G. 2016. Thiolato-bridged dinuclear arene ruthenium complexes and their potential as anticancer drugs. Coord Chem Rev 309:36-50. http://dx.doi.org/10.1016/j.ccr.2015.10.007

22. Tomsik P, Muthna D, Rezacova M, Micuda S, Cmielova J, Hroch M, Endlicher R, Cervinkova Z, Rudolf E, Hann S, Stibal D, Therrien B, Süss-Fink G. 2015. (p-MeC6H4Pri)(2)Ru-2(SC6H4-p-Bu-t)(3) Cl (diruthenium-1), a dinuclear arene ruthenium compound with very high anticancer activity: An in vitro and in vivo study. J Organomet Chem 782:42-51. 10.1016/j.jorganchem.2014.10.050

23. Li F, Collins JG, Keene FR. 2015. Ruthenium complexes as antimicrobial agents. Chem Soc Rev 44:2529-2542. 10.1039/c4cs00343h

24. Barna F, Debache K, Vock CA, Küster T, Hemphill A. 2013. In Vitro Effects of Novel Ruthenium Complexes in Neospora caninum and Toxoplasma gondii Tachyzoites. Antimicrob Agents Chemother 57:5747-5754. 10.1128/aac.02446-12

25. Hess J, Keiser J, Gasser G. 2015. Toward organometallic antischistosomal drug candidates. Future Med Chem 7:821-830. 10.4155/fmc.15.22

26. Kljun J, Scott AJ, Lanišnik Rižner T, Keiser J, Turel I. 2014. Synthesis and Biological Evaluation of Organoruthenium Complexes with Azole Antifungal Agents. First Crystal Structure of a Tioconazole Metal Complex. Organometallics 33:1594-1601. 10.1021/om401096y

27. Küster T, Lense N, Barna F, Hemphill A, Kindermann MK, Heinicke JW, Vock CA. 2012. A New Promising Application for Highly Cytotoxic Metal Compounds: η6-Areneruthenium(II) Phosphite Complexes for the Treatment of Alveolar Echinococcosis. J Med Chem 55:4178-4188. 10.1021/jm300291a

28. Martínez A, Carreon T, Iniguez E, Anzellotti A, Sánchez A, Tyan M, Sattler A, Herrera L, Maldonado RA, Sánchez-Delgado RA. 2012. Searching for New Chemotherapies for Tropical Diseases: Ruthenium–Clotrimazole Complexes Display High in Vitro Activity against Leishmania major and Trypanosoma cruzi and Low Toxicity toward Normal Mammalian Cells. J Med Chem 55:3867-3877. 10.1021/jm300070h

29. Keiser J, Vargas M, Rubbiani R, Gasser G, Biot C. 2014. In vitro and in vivo antischistosomal activity of ferroquine derivatives. Parasites & Vectors 7:1-7. 10.1186/1756-3305-7-424

30. Biot C, Dive D. 2010. Bioorganometallic Chemistry and Malaria, p 155-193. *In* Jaouen G, Metzler-Nolte N (ed), Medicinal Organometallic Chemistry. Springer Berlin Heidelberg, Berlin, Heidelberg.

31. Beagley P, Blackie MAL, Chibale K, Clarkson C, Moss JR, Smith PJ. 2002. Synthesis and antimalarial activity in vitro of new ruthenocene-chloroquine analogues. Journal of the Chemical Society, Dalton Transactions:4426-4433. 10.1039/b205432a
32. Smith GS, Therrien B. 2011. Targeted and multifunctional arene ruthenium chemotherapeutics. Dalton Trans 40:10793-10800. 10.1039/c1dt11007a
33. Ali MI, Rauf MK, Badshah A, Kumar I, Forsyth CM, Junk PC, Kedzierski L, Andrews PC. 2013. Anti-leishmanial activity of heteroleptic organometallic Sb(v) compounds. Dalton Trans 42:16733-16741. 10.1039/c3dt51382c
34. Simpson PV, Schmidt C, Ott I, Bruhn H, Schatzschneider U. 2013. Synthesis, Cellular Uptake and Biological Activity Against Pathogenic Microorganisms and Cancer Cells of Rhodium and Iridium N-Heterocyclic Carbene Complexes Bearing Charged Substituents. Eur J Inorg Chem 2013:5547-5554. 10.1002/ejic.201300820
35. Maia PIdS, Carneiro ZR, Lopes CD, Oliveira CG, Silva JS, Albuquerque S, Hagenbach A, Gust R, Deflon V, Abram U. 2017. Organometallic Gold(III) Complexes with Hybrid SNS-Donating Thiosemicarbazone Ligands: Cytotoxicity and anti-Trypanosoma cruzi Activity. Dalton Trans. 10.1039/c6dt04307k
36. Clède S, Cowan N, Lambert F, Bertrand HC, Rubbiani R, Patra M, Hess J, Sandt C, Trcera N, Gasser G, Keiser J, Policar C. 2016. Bimodal X-ray and Infrared Imaging of an Organometallic Derivative of Praziquantel in Schistosoma mansoni. ChemBioChem 17:1004-1007. 10.1002/cbic.201500688
37. Hess J, Patra M, Jabbar A, Pierroz V, Konatschnig S, Spingler B, Ferrari S, Gasser RB, Gasser G. 2016. Assessment of the nematocidal activity of metallocenyl analogues of monepantel. Dalton Trans 45:17662-17671. 10.1039/c6dt03376h
38. Hess J, Patra M, Pierroz V, Spingler B, Jabbar A, Ferrari S, Gasser RB, Gasser G. 2016. Synthesis, Characterization, and Biological Activity of Ferrocenyl Analogues of the Anthelmintic Drug Monepantel. Organometallics 35:3369-3377. 10.1021/acs.organomet.6b00577
39. Hess J, Patra M, Rangasamy L, Konatschnig S, Blacque O, Jabbar A, Mac P, Jorgensen EM, Gasser RB, Gasser G. 2016. Organometallic Derivatization of the Nematocidal Drug Monepantel Leads to Promising Antiparasitic Drug Candidates. Chem--Eur J 22:16602-16612. 10.1002/chem.201602851
40. Patra M, Ingram K, Leonidova A, Pierroz V, Ferrari S, Robertson MN, Todd MH, Keiser J, Gasser G. 2013. In Vitro Metabolic Profile and in Vivo Antischistosomal Activity Studies of (η6-Praziquantel)Cr(CO)3 Derivatives. J Med Chem 56:9192-9198. 10.1021/jm401287m
41. Patra M, Ingram K, Pierroz V, Ferrari S, Spingler B, Gasser RB, Keiser J, Gasser G. 2013. [(η6-Praziquantel)Cr(CO)3] Derivatives with Remarkable In Vitro Anti-schistosomal Activity. Chem--Eur J 19:2232-2235. 10.1002/chem.201204291
42. Nuralitha S, Siregar JE, Syafruddin D, Roelands J, Verhoef J, Hoepelman AIM, Marzuki S. 2015. Within-Host Selection of Drug Resistance in a Mouse Model of Repeated Incomplete Malaria Treatment: Comparison between Atovaquone and Pyrimethamine. Antimicrob Agents Chemother. 10.1128/aac.00538-15
43. Simpson PV, Nagel C, Bruhn H, Schatzschneider U. 2015. Antibacterial and Antiparasitic Activity of Manganese(I) Tricarbonyl Complexes with Ketoconazole, Miconazole, and Clotrimazole Ligands. Organometallics 34:3809-3815. 10.1021/acs.organomet.5b00458
44. Halonen SK, Weiss LM. 2013. Chapter 8 - Toxoplasmosis, p 125-145. *In* Hector H. Garcia HBT, Oscar HDB (ed), Handbook of Clinical Neurology, vol Volume 114. Elsevier.
45. Kaye A. 2011. Toxoplasmosis: Diagnosis, Treatment, and Prevention in Congenitally Exposed Infants. J Pediatr Health Care 25:355-364. 10.1016/j.pedhc.2010.04.008

46. Fichera ME, Roos DS. 1997. A plastid organelle as a drug target in apicomplexan parasites. Nature 390:407-409.
47. Stíbal D, Therrien B, Süss-Fink G, Nowak-Sliwinska P, Dyson PJ, Čermáková E, Řezáčová M, Tomšík P. 2016. Chlorambucil conjugates of dinuclear p-cymene ruthenium trithiolato complexes: synthesis, characterization and cytotoxicity study in vitro and in vivo. JBIC Journal of Biological Inorganic Chemistry 21:443-452. 10.1007/s00775-016-1353-z
48. Stibal D, Therrien B, Giannini F, Paul LEH, Furrer J, Suss-Fink G. 2014. Monothiolato-Bridged Dinuclear Arene Ruthenium Complexes: The Missing Link in the Reaction of Arene Ruthenium Dichloride Dimers with Thiols. Eur J Inorg Chem:5925-5931. 10.1002/ejic.201402754
49. Ibao A-F, Gras M, Therrien B, Süss-Fink G, Zava O, Dyson PJ. 2012. Thiolato-Bridged Arene–Ruthenium Complexes: Synthesis, Molecular Structure, Reactivity, and Anticancer Activity of the Dinuclear Complexes [(arene)2Ru2(SR)2Cl2]. Eur J Inorg Chem 2012:1531-1535. 10.1002/ejic.201101057
50. McFadden DC, Seeber F, Boothroyd JC. 1997. Use of Toxoplasma gondii expressing beta-galactosidase for colorimetric assessment of drug activity in vitro. Antimicrob Agents Chemother 41:1849-1853.
51. Müller J, Hemphill A. 2013. Chapter Seven - New Approaches for the Identification of Drug Targets in Protozoan Parasites, p 359-401. *In* Kwang WJ (ed), Int Rev Cell Mol Biol, vol Volume 301. Academic Press.
52. Klinkert MQ, Heussler V. 2006. The Use of Anticancer Drugs in Antiparasitic Chemotherapy. Mini-Rev Med Chem 6:131-143. http://dx.doi.org/10.2174/138955706775475939
53. Ojo KK, Reid MC, Kallur Siddaramaiah L, Müller J, Winzer P, Zhang Z, Keyloun KR, Vidadala RSR, Merritt EA, Hol WGJ, Maly DJ, Fan E, Van Voorhis WC, Hemphill A. 2014. <italic>Neospora caninum</italic> Calcium-Dependent Protein Kinase 1 Is an Effective Drug Target for Neosporosis Therapy. PLoS One 9:e92929. 10.1371/journal.pone.0092929
54. Kropf C, Debache K, Rampa C, Barna F, Schorer M, Stephens CE, Ismail MA, Boykin DW, Hemphill A. 2012. The adaptive potential of a survival artist: characterization of the in vitro interactions of Toxoplasma gondii tachyzoites with di-cationic compounds in human fibroblast cell cultures. Parasitology 139:208-220. Doi: 10.1017/s0031182011001776
55. Ojo KK, Reid MC, Kallur Siddaramaiah L, Müller J, Winzer P, Zhang Z, Keyloun KR, Vidadala RS, Merritt EA, Hol WG, Maly DJ, Fan E, Voorhis WC, Hemphill A. 2014. Neospora caninum calcium-dependent protein kinase 1 is an effective drug target for neosporosis therapy. PLoS One 9. 10.1371/journal.pone.0092929
56. Müller J, Aguado-Martinez A, Manser V, Balmer V, Winzer P, Ritler D, Hostettler I, Solís D, Ortega-Mora LM, Hemphill A. 2015. Buparvaquone is active against Neospora caninum in vitro and in experimentally infected mice. Int J Parasitol Drugs Drug Resist 5. 10.1016/j.ijpddr.2015.02.001
57. Winzer P, Müller J, Aguado-Martínez A, Rahman M, Balmer V, Manser V, Ortega-Mora LM, Ojo KK, Fan E, Maly DJ, Van Voorhis WC, Hemphill A. 2015. In Vitro and In Vivo Effects of the Bumped Kinase Inhibitor 1294 in the Related Cyst-Forming Apicomplexans Toxoplasma gondii and Neospora caninum. Antimicrob Agents Chemother 59:6361-6374. 10.1128/aac.01236-15
58. Syafruddin D, Siregar JE, Marzuki S. 1999. Mutations in the cytochrome b gene of Plasmodium berghei conferring resistance to atovaquone. Mol Biochem Parasitol 104:185-194. http://dx.doi.org/10.1016/S0166-6851(99)00148-6

59. McFadden DC, Tomavo S, Berry EA, Boothroyd JC. 2000. Characterization of cytochrome b from Toxoplasma gondii and Qo domain mutations as a mechanism of atovaquone-resistance. Mol Biochem Parasitol 108:1-12. http://dx.doi.org/10.1016/S0166-6851(00)00184-5

60. Sharifiyazdi H, Namazi F, Oryan A, Shahriari R, Razavi M. 2012. Point mutations in the Theileria annulata cytochrome b gene is associated with buparvaquone treatment failure. Veterinary Parasitology 187:431-435. http://dx.doi.org/10.1016/j.vetpar.2012.01.016

61. Marsolier J, Perichon M, DeBarry JD, Villoutreix BO, Chluba J, Lopez T, Garrido C, Zhou XZ, Lu KP, Fritsch L, Ait-Si-Ali S, Mhadhbi M, Medjkane S, Weitzman JB. 2015. Theileria parasites secrete a prolyl isomerase to maintain host leukocyte transformation. Nature 520:378-382. 10.1038/nature14044

62. Yousif LF, Stewart KM, Kelley SO. 2009. Targeting Mitochondria with Organelle-Specific Compounds: Strategies and Applications. ChemBioChem 10:1939-1950. 10.1002/cbic.200900185

63. Chen LB. 1988. Mitochondrial Membrane Potential in Living Cells. Annu Rev Cell Biol 4:155-181. doi:10.1146/annurev.cb.04.110188.001103

64. Mulcahy SP, Grundler K, Frias C, Wagner L, Prokop A, Meggers E. 2010. Discovery of a strongly apoptotic ruthenium complex through combinatorial coordination chemistry. Dalton Trans 39:8177-8182. 10.1039/c0dt00034e

65. Pierroz V, Joshi T, Leonidova A, Mari C, Schur J, Ott I, Spiccia L, Ferrari S, Gasser G. 2012. Molecular and Cellular Characterization of the Biological Effects of Ruthenium(II) Complexes Incorporating 2-Pyridyl-2-pyrimidine-4-carboxylic Acid. J Am Chem Soc 134:20376-20387. 10.1021/ja307288s

66. Li L, Wong Y-S, Chen T, Fan C, Zheng W. 2012. Ruthenium complexes containing bis-benzimidazole derivatives as a new class of apoptosis inducers. Dalton Trans 41:1138-1141. 10.1039/c1dt11950h

67. Wang J-Q, Zhang P-Y, Qian C, Hou X-J, Ji L-N, Chao H. 2014. Mitochondria are the primary target in the induction of apoptosis by chiral ruthenium(II) polypyridyl complexes in cancer cells. J Biol Inorg Chem 19:335-348. 10.1007/s00775-013-1069-2

68. Jacot D, Waller RF, Soldati-Favre D, MacPherson DA, MacRae JI. 2016. Apicomplexan Energy Metabolism: Carbon Source Promiscuity and the Quiescence Hyperbole. Trends in Parasitology 32:56-70. https://doi.org/10.1016/j.pt.2015.09.001

69. Kristensen R, Torp M, Kosiak B, Holst-Jensen A. 2005. Phylogeny and toxigenic potential is correlated in Fusarium species as revealed by partial translation elongation factor 1 alpha gene sequences. Mycol Res 109:173-186. http://dx.doi.org/10.1017/S0953756204002114

70. Ridgley EL, Xiong Z-h, Kaur KJ, Ruben L. 1996. Genomic organization and expression of elongation factor-1α genes in Trypanosoma brucei. Mol Biochem Parasitol 79:119-123. http://dx.doi.org/10.1016/0166-6851(96)02639-4

71. Toueille M, Saint-Jean B, Castroviejo M, Benedetto J-P. 2007. The elongation factor 1A: A novel regulator in the DNA replication/repair protein network in wheat cells? Plant Physiology and Biochemistry 45:113-118. https://doi.org/10.1016/j.plaphy.2007.01.006

72. Lamberti A, Longo O, Marra M, Tagliaferri P, Bismuto E, Fiengo A, Viscomi C, Budillon A, Rapp UR, Wang E, Venuta S, Abbruzzese A, Arcari P, Caraglia M. 2007. C-Raf antagonizes apoptosis induced by IFN-[alpha] in human lung cancer cells by phosphorylation and increase of the intracellular content of elongation factor 1A. Cell Death Differ 14:952-962. http://www.nature.com/cdd/journal/v14/n5/suppinfo/4402102s1.html

73. Bouzaidi-Tiali N, Aeby E, Charrière F, Pusnik M, Schneider A. 2007. Elongation factor 1a mediates the specificity of mitochondrial tRNA import in T. brucei. The EMBO Journal 26:4302-4312. 10.1038/sj.emboj.7601857

74. Esseiva AC, Naguleswaran A, Hemphill A, Schneider A. 2004. Mitochondrial tRNA Import in Toxoplasma gondii. J Biol Chem 279:42363-42368. 10.1074/jbc.M404519200

75. Matsubayashi M, Teramoto-Kimata I, Uni S, Lillehoj HS, Matsuda H, Furuya M, Tani H, Sasai K. 2013. Elongation Factor-1α Is a Novel Protein Associated with Host Cell Invasion and a Potential Protective Antigen of Cryptosporidium parvum. J Biol Chem 288:34111-34120. 10.1074/jbc.M113.515544

76. Wang S, Zhang Z, Wang Y, Gadahi JA, Xu L, Yan R, Song X, Li X. 2017. Toxoplasma gondii Elongation Factor 1-Alpha (TgEF-1α) Is a Novel Vaccine Candidate Antigen against Toxoplasmosis. Frontiers in Microbiology 8. 10.3389/fmicb.2017.00168

77. Wang S, Wang Y, Sun X, Zhang Z, Liu T, Gadahi JA, Hassan IA, Xu L, Yan R, Song X, Li X. 2015. Protective immunity against acute toxoplasmosis in BALB/c mice induced by a DNA vaccine encoding Toxoplasma gondii elongation factor 1-alpha. BMC Infectious Diseases 15:448. 10.1186/s12879-015-1220-5

665 **Figure legends**

666 **FIG. 1.** Structures of complexes 1-18 used in this study. Note that compounds 1, 2 and 9 were
667 further characterized.

668

669 **FIG. 2.** Ultrastructure of *T. gondii* tachyzoites grown in HFF. A is a low magnification view
670 of infected HFF, the boxed area is shown at a higher magnification in B. Tachyzoites
671 proliferate within a parasitiophorous vacuole, surrounded by a parasitophorous vacuole
672 membrane. Nuc = nucleus, dg = dense granules, mic = micronemes, rop = rhoptries, mito =
673 mitochondrion. The boxed area in B shows the mitochondrial matrix and is enlarged in C. Bar
674 in A = 1.8 µm, B = 0.3 µm, C = 0.1 µm

675

676 **FIG. 3.** Ultrastructure of *T. gondii* tachyzoites grown in HFF and treated with ruthernium
677 compounds 1 and 9. Treatments were carried out using 200 nM of compounds 1 (A-D) or 9
678 (E, F). A is a low magnification view of parasites treated with compound 1for 6 h, the boxed
679 areas are enlarged in B and C. D shows parasites exposed to compound 1 for 48 h. E and F
680 show parasites exposed to compound 9 during 24 h. Note the distinct alterations in the
681 mitochondria (mito) in B, C and E, and the still intact host cell mitochondria (h-mito) in D¨.
682 The boxed area in F is enlarged in E. Bar in A, F = 1 µm, B, C, E = 0.4 µm, D = 0.8 µm,

683

684 **FIG. 4.** Compound 9 inhibits *T. gondii* tachyzoite proliferation only when applied early
685 during infection. HFF monolayers grown in 96 well plates were treated with compound 9
686 (100 nM) either 10 min prior to infection or 1 h, 5 h or 24 h post-infection with *T. gondii*
687 tachyzoites. The proliferation of tachyzoites was measured after 2 days of culture by beta-
688 galactosidase assay as described in materials and methods

689

690 **FIG. 5.** Identification of complex 9-binding proteins. A, SDS-PAGE and silver staining of
691 tandem (mock- and compound 9-sepharose) affinity chromatography of a protein extract
692 prepared from *T. gondii* infected HFF. Soluble extract and non-binding fraction (flow-
693 through) are shown on the left, followed by wash and eluate fractions of the mock columns
694 and the complex 9-sepharose column. The two arrows point to the two bands of 50 kda and
695 20 kDa, which were cut out and analyzed by LC-MS. B shows the amino acid sequence of the
696 50 kDa band identified as TgEF1-alpha, the peptide sequences identified by LC-MS are
697 underlined.
698

Tables

Table 1. The efficacies of dinuclear thiolate-bridged arene ruthenium complexes against *T. gondii* beta-galactosidase expressing tachyzoites, host cell (HFF) cytotoxicity, and respective physicochemical data. Chloride salts of the corresponding thiols of the complexes [1-6] were used for all experiments. For the determination of efficacies, confluent HFF monolayers grown in a 96-well plate were treated with the complexes at various concentrations, and were infected with *T. gondii* beta-gal tachyzoites (10^3 per well). After 3 days, beta-galactosidase activity or host cell viability were determined, IC_{50} values were calculated as described, and are presented with 95% confidence intervals. The LogP values correspond to the values that were calculated for the thiols RSH groups [ref17]. nd = not done

Complex	*T. gondii* beta-gal IC_{50} (nM)	HFF IC_{50} (µM)	LogP *(RSH)*
1	34 ± 4	800	2.98 ± 0.28
2	62 ± 10	>1000	4.21 ± 0.29
3	130 ± 20	nd	2.38 ± 0.32
4	120 ± 20	nd	2.83 ± 0.42
5	540 ± 60	nd	1.68 ± 0.29
9	1.2 ± 0.5	5‘129	nd

717 Table 2. Results of mass spectrometry analysis of the two major bands shown in Fig. 5. AC, UniProt accession number; ID, UniProt identifier;

718 PMSS, protein match score summation.

Band	AC	ID	PMSS	Protein Score	unique peptides	Coverage (%)	Protein Mass (Da)	Description
20 kDa	P46783	RS10_HUMAN	79	147	5	32.7	18898	40S ribosomal protein S10
	P30050	RL12_HUMAN	72	161	5	43.0	17819	60S ribosomal protein L12
	S8FA78	S8FA78_TOXGO	46	86	3	25.5	17821	Ribosomal protein RPL12
	V4YUP9	V4YUP9_TOXGO	30	69	3	21.8	16331	Ribosomal protein RPL27
	P62269	RS18_HUMAN	29	67	3	19.1	17719	40S ribosomal protein S18
	S8EUB1	S8EUB1_TOXGO	26	61	3	21.8	17723	Ribosomal protein RPS18
	P61254	RL26_HUMAN	25	55	3	16.6	17258	60S ribosomal protein L26
	P62851	RS25_HUMAN	24	35	2	13.6	13742	40S ribosomal protein S25
	Q5SGD8	Q5SGD8_TOXGO	18	37	2	11.1	19983	Tgd057
50 kDa	S8GV85	S8GV85_TOXGO	323	518	17	47.5	49006	Elongation factor 1-alpha
	P68104	EF1A1_HUMAN	143	196	8	22.9	50141	Elongation factor 1-alpha 1
	O14773-2	TPP1_HUMAN	71	120	5	27.2	34464	Isoform 2 of Tripeptidyl-peptidase 1
	P63261	ACTG_HUMAN	36	77	4	14.7	41793	Actin, cytoplasmic 2
	P06576	ATPB_HUMAN	32	61	3	8.3	56560	ATP synthase subunit beta, mitochondrial
	P22234	PUR6_HUMAN	26	47	2	6.1	47079	Multifunctional protein ADE2
	P16989-2	YBOX3_HUMAN	22	42	2	8.3	31947	Isoform 2 of Y-box-binding protein 3
	O75821	EIF3G_HUMAN	18	32	2	5.0	35611	Eukaryotic translation initiation factor 3 subunit G
	Q9Y6N5	SQRD_HUMAN	17	31	2	6.2	49961	Sulfide:quinone oxidoreductase, mitochondrial

719

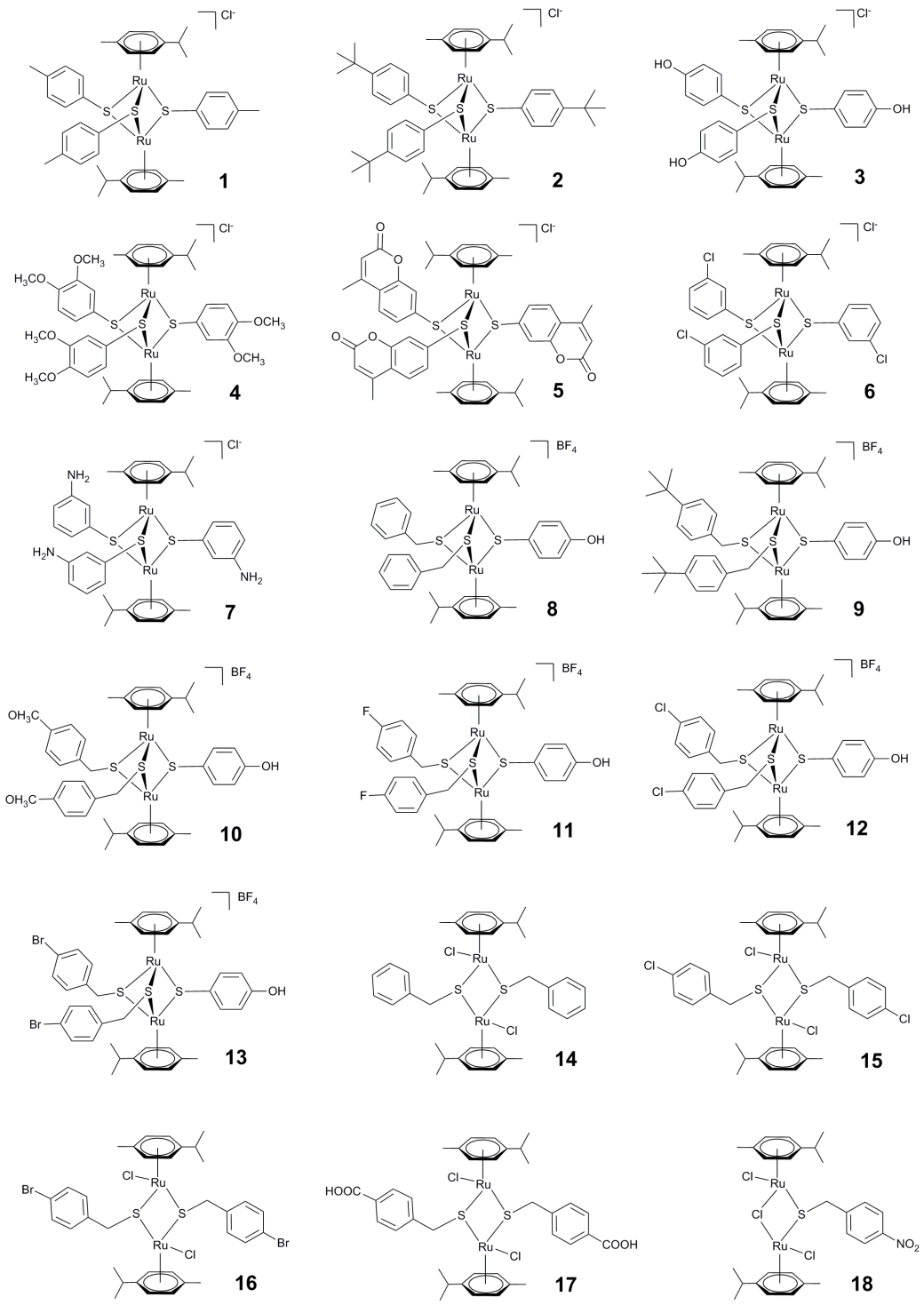

FIG. 1. Structures of complexes 1-18 used in this study. Not that compounds 1, 2 and 9 were further characterized.

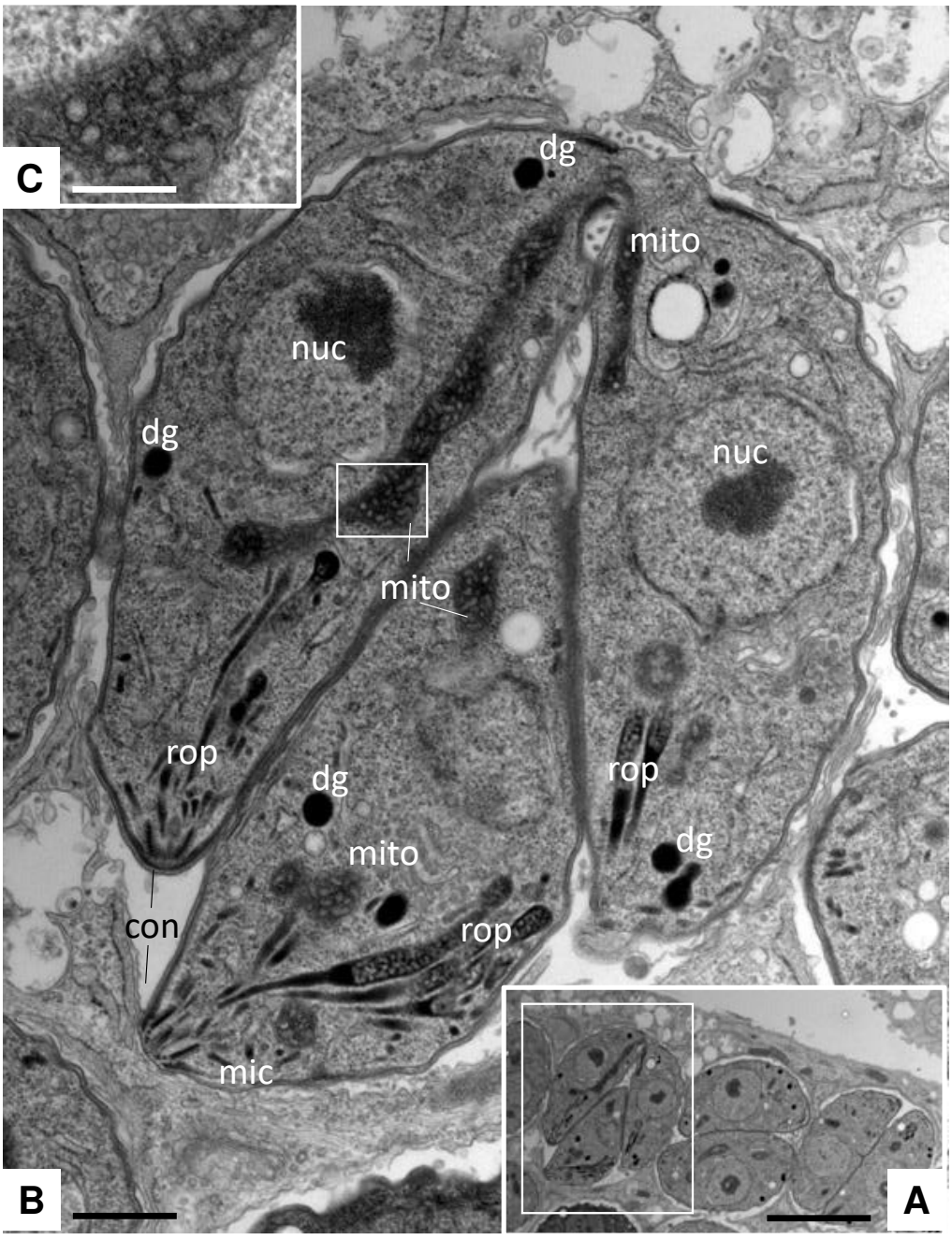

FIG. 2. Ultrastructure of *T. gondii* tachyzoites grown in HFF. A is a low magnification view of infected HFF, the boxed area is shown at a higher magnification in B. Tachyzoites proliferate within a parasitiophorous vacuole, surrounded by a parasitophorous vacuole membrane. Nuc = nucleus, dg = dense granules, mic = micronemes, rop = rhoptries, mito = mitochondrion. The boxed area in B shows the mitochondrial matrix and is enlarged in C. Bar in A = 1.8 µm, B = 0.3 µm, C = 0.1 µm

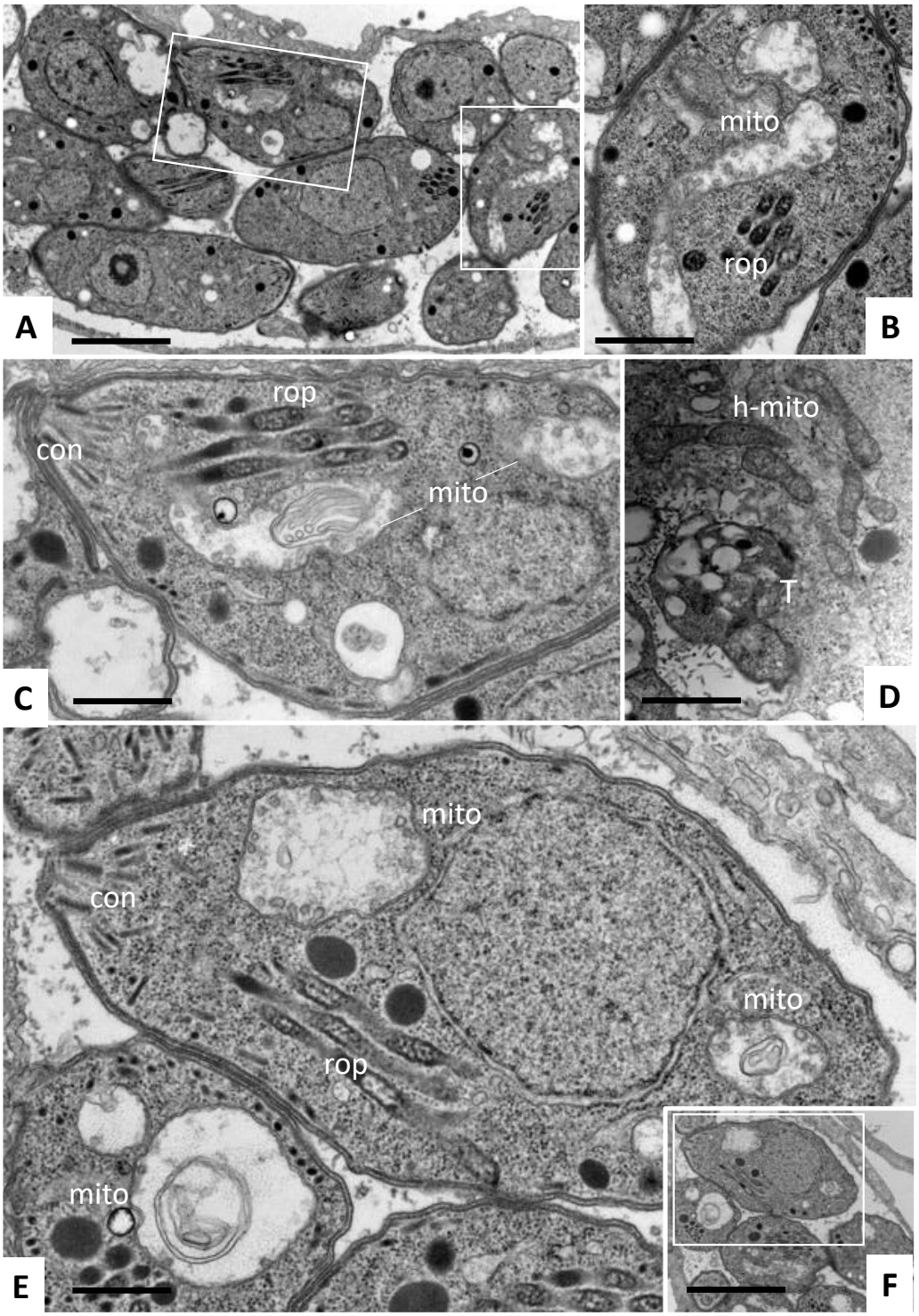

FIG. 3. Ultrastructure of *T. gondii* tachyzoites grown in HFF and treated with ruthernium compounds 1 and 9. Treatments were carried out using 200 nM of compounds 1 (A-D) or 9 (E, F). A is a low magnification view of parasites treated with compound 1for 6 h, the boxed areas are enlarged in B and C. D shows parasites exposed to compound 1 for 48 h. E and F show parasites exposed to compound 9 during 24 h. Note the distinct alterations in the mitochondria (mito) in B, C and E, and the still intact host cell mitochondria (h-mito) in D¨. The boxed area in F is enlarged in E. Bar in A, F = 1 µm, B, C, E = 0.4 µm, D = 0.8 µm,

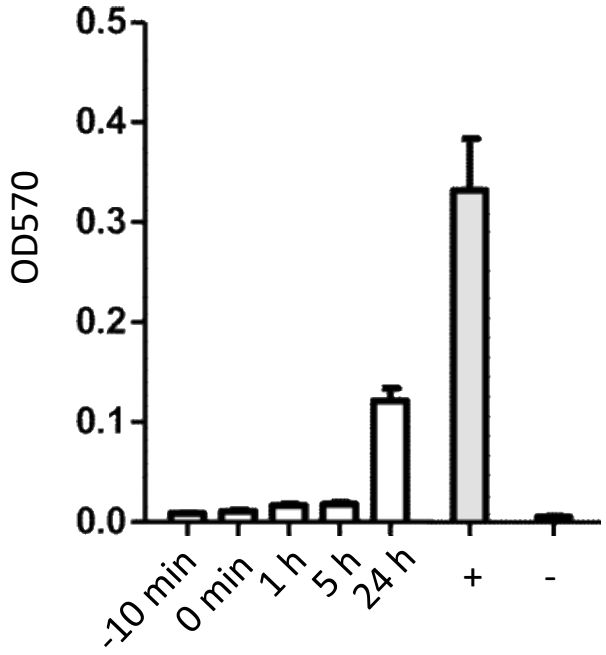

FIG. 4. Compound 9 inhibits *T. gondii* tachyzoite proliferation only when applied early during infection. HFF monolayers grown in 96 well plates were treated with compound 9 (100 nM) either 10 min prior to infection or 1 h, 5 h or 24 h post-infection with *T. gondii* tachyzoites. The proliferation of tachyzoites was measured after 2 days of culture by beta-galactosidase assay as described in materials and methods

A

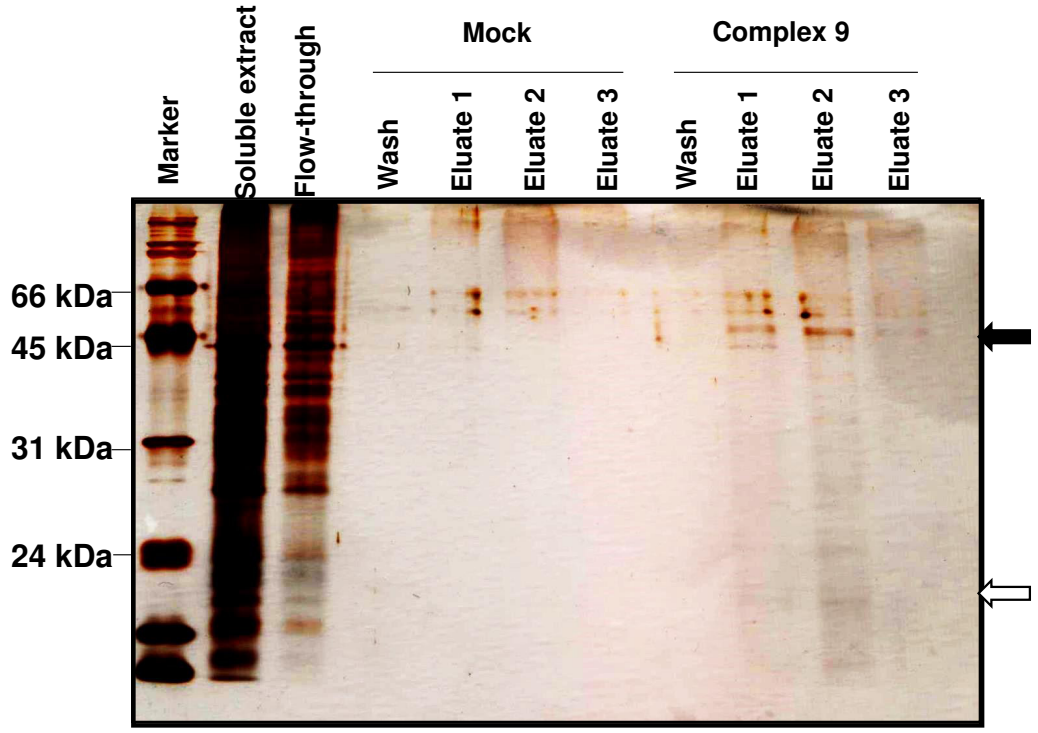

B

MGKEKTHINLVVIGHVDSGKSTTTGHLIYKLGGIDKRTIEKFEKESSEMGKGSFKYAWVL
DKLKAERERGITIDIALWQFETPKYHYTVIDAPGHRDFIKNMITGTSQADVALLVVPAEA
GGFEGAFSKEGQTREHALLAFTLGVKQMIVGINKMDSCNYSEDRFNEIQKEVAMYLKKVG
YNPEKVPFVAISGFVGDNMVEKSTNMSWYKGKTLVEALDTMEAPKRPSDKPLRLPLQDVY
KIGGIGTVPVGRVETGILKAGMVLTFAPVGLTTECKSVEMHHEVMEQAVPGDNVGFNVKN
VSVKELKRGYVASDSKNDPAKGCATFLAQVIVLNHPGEIKNGYSPVIDCHTAHIACKFAE
IKTKMDKRSGKTLEEAPKCIKSGDAAMVNMEPSKPMVVEAFTDYPPLGRFAVRDMKQTVA
VGVIKSVEKKEPGAGSKVTKSAVKAAKK

FIG. 5. Identification of complex 9-binding proteins. A, SDS-PAGE and silver staining of tandem (mock- and compound 9-sepharose) affinity chromatography of a protein extract prepared from *T. gondii* infected HFF. Soluble extract and non-binding fraction (flow-through) are shown on the left, followed by wash and eluate fractions of the mock columns and the complex 9-sepharose column. The two arrows point to the two bands of 50 kd and 20 kDa, which were cut out and analyzed by LC-MS. B shows the peptide sequence of TgEF1-alpha, the peptide sequences identified by LC-MS are underlined.